

Figure S1. TPN-II cold responses are driven by antennal sensory neurons. Related to Figure 2.

(A-B) Persistent firing in TPN-II neurons at stable cold temperature. (A) Two representative current clamp recordings from TPN-II neurons in response to a -3°C temperature step. (B) Firing rate histogram from N=8 cells; black trace and gray shading indicate $av \pm SEM$; stimulus: blue trace at the bottom of B, $av \pm SEM$. (C) Overlay of green fluorescence with a DotD contrast image acquired under 2-photon microscopy, illustrating the location of TPN-IIs (expressing GFP) in relation to the antennal nerve. Scissors and hashed line indicate the region of the antennal nerve targeted for acute resection. (D-E) Acute antennal nerve resection abolishes cold-driven responses in TPN-II. (D) Two representative current clamp recordings from TPN-II neurons after antennal nerve resection, challenged with a -3°C temperature step as in A-B (blue, bottom in E). (E) Firing rate histogram from N=5 cells; black trace and gray shading indicate $av \pm SEM$; stimulus: blue trace at the bottom of E, $av \pm SEM$. Scale bar in C=50 μ m.

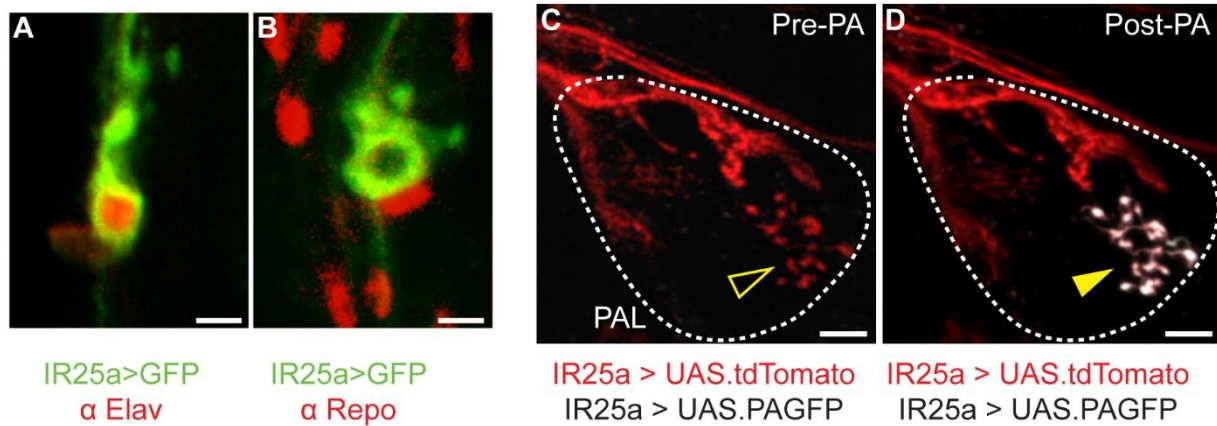


Figure S2. Characterization of Anterior Cold cells. Related to Figure 3.

(**A-B**) IR25a>GFP labels Anterior Cold cell (ACc) in the antennal nerve. ACc expresses the neuron-specific marker, Elav (**A**, red), and does not express the glial-specific marker, Repo (**B**, red; panels are maximum-intensity projections of shallow confocal stacks acquired from immunostained whole-mount brains, Scale bar = 5 μ m). (**C,D**) Photoactivation of PA-GFP identifies terminals of ACc in the cold glomerulus of the PAL. (**C**) Ablation of the antenna in an IR25a>tdTomato animal reveals residual innervation of the cold glomerulus of the PAL (see also **Figure 3**). Note that **C** is an ipsi-lateral ablation performed one week prior to imaging. Here, with the exception of the cold glomerulus, the PAL volume is void of IR25a projections (the red diagonal fibers atop the PAL come from contralateral innervation, and –unlike the residual innervation of the cold glomerulus, degenerate in bi-lateral ablation experiments). (**D**) Following photo-activation of ACc cell bodies (co-expressing PA-GFP under IR25a-Gal4), GFP fluorescence can be traced to terminals in the cold glomerulus (scale bars in **C,D** 20 μ m).

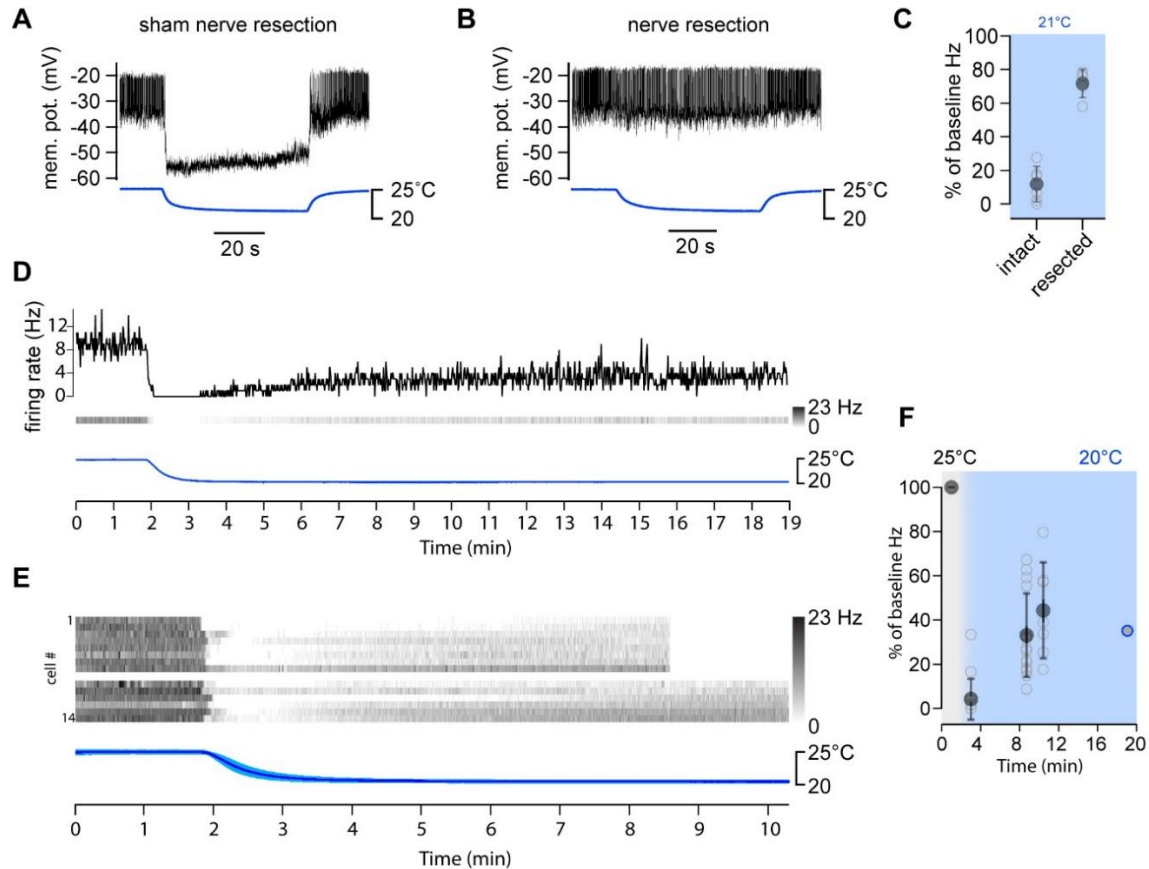


Figure S3. Persistent inhibition of DN1a neurons by cold. Related to Figure 5.

DN1a inhibition by cold temperature is largely abolished by acute antennal nerve resection (removing all antennal sensory neurons and likely removing/damaging ACcs). **(A)** Representative whole-cell current clamp recording from a DN1a neuron following sham treatment (stimulus: blue trace; see Figure 5 for additional normal responses). **(B)** Representative whole-cell current clamp recording from a DN1a neuron following nerve resection (stimulus: blue trace). **(C)** Quantification of reduction in DN1a firing rate (as % of baseline Hz) from a 4°C (blue shading) cooling step in intact or resected brains, recorded at ZT4-8 (N=5 cells each). Open circles are quantifications from individual neurons. Filled circles indicate $av \pm SD$. **(D-F)** DN1a firing rates in constant cold temperature do not recover to baseline firing rates. **(D)** Firing rate histogram (black) in response to constant cold conditions (blue trace) from a single neuron recorded continuously for at least ~20 min. Pseudo-colored spike rate histogram (middle) of the above cell (white indicates periods of neuronal silencing). **(E)** Pseudocolored firing rate histograms for additional DN1a neurons in response to stable cold conditions (blue trace) for either ~8.5 (top) or ~10 minutes (bottom; temperature trace is av of $6 \pm SD$). **(F)** Quantification of reduction in firing rate of DN1a neurons at 25°C and in response to stable cold conditions (20°C, blue shading) at different time points. Open circles indicate inhibition of individual neurons, filled circles represent the $av \pm SD$. Filled circle with blue outline is the quantification for the response in **(D)**.

Figure	Genotype	panel	
1	19428 Gal4/ UAS.Gcamp6f	B	
	49B06 Gal4/ UAS.Gcamp6f	C	
	49B06 Gal4/ UAS.CD8::GFP	D-J	
2	49B06 Gal4/ UAS.CD8::GFP	A-F	
3	25B07AD; 77C10DBD/ UAS.CD8::GFP	C,D	
	25B07 LexA/ Aop.CD2::GFP	E,F	
	IR25a Gal4/ UAS.CD8::GFP	G,H	
	60H12 AD; VT032805 DBD/ UAS.CD8::GFP	I	
	49B06 LexA/ Aop.CD2::GFP; 77C10 Gal4/ UAS.TdTomato	J-L	
	25B07 LexA/ Aop.CD2::GFP; 77C10 Gal4/ UAS.TdTomato	M-O	
	25B07 LexA/ AOP.Syb:spGFP[1-0]; 49B06 Gal4/ UAS.spGFP[11]	P	
	49B06 LexA/ Aop.spGFP[11]; 77C10 Gal4/ UAS.Syb:spGFP[1-0]	Q-R	
	25B07AD; 77C10DBD/ UAS.Gcamp7f	S	
	25B07 LexA/ Aop.Gcamp7f	T	
	Ir25a Gal4/ UAS.Gcamp7f	U	
	4	Aop.TdTomato; 49B06 LexA/UAS.SPA; nSyb Gal4	B,C
		49A06 Gal4/ UAS.CD8::GFP	D-M
49B06 LexA/ AOP.Syb:spGFP[1-0]; VT03226 Gal4/ UAS.spGFP[11]		O	
5	49A06 Gal4/ UAS.CD8::GFP	B	
	49B06 Gal4/ UAS.CD8::GFP	C	
	VT032226/ UAS.CD8::GFP	D-F,I-K,M,N	
	60H12 Gal4/ UAS.CD8::GFP	G	
	per ⁰¹ ;VT032226/ UAS.CD8::GFP	L	
6	WT	A-D	
	23E05 AD; 92H07 DBD/ UAS.CD8::GFP	E	
	23E05 AD; 92H07 DBD/ +	F,H	
	23E05 AD; 92H07 DBD/ UAS.TNT	G,H	
	UAS.TNT/ +	H,I,L	
	60H12 AD; VT032805 DBD/+	J,L	
	60H12 AD; VT032805 DBD/ UAS.TNT	K,L	
7	WT	A,B	
	23E05AD ;92H07 DBD/ +	C-E	
	UAS.TNT/ +	C-E	
	23E05AD ;92H07 DBD/ UAS.TNT	C-E	
	60H12 AD; VT032805 DBD/ UAS.CsChrimson	G-I	
	VT03226 Gal4/ UAS.CD8::GFP	K,L,R-T	
	PDF LexA/ Aop.P2X2; 23E05 Gal4/ UAS.CD8::GFP	N-P	
S1	49B06 Gal4 / UAS.CD8::GFP	A,B	
	60H12AD;VT032805DBD/ UAS.CD8::GFP	C-E	
S2	IR25a Gal4/ UAS.CD8::GFP	A-B	
	IR25a Gal4/ UAS.TdTomato; UAS C3PA	C,D	
S3	23E05 Gal4 / UAS.CD8::GFP	A-F	

Table S1. Genotypes used in this study. Related to STAR Methods